

# Local temperature control of photonic crystal devices via micron-scale electrical heaters

Andrei Faraon<sup>a)</sup> and Jelena Vučković

*E. L. Ginzton Laboratory, Stanford University, Stanford, California 94305, USA*

(Received 27 April 2009; accepted 2 July 2009; published online 27 July 2009)

We demonstrate a method to locally control the temperature of photonic crystal devices via micron-scale electrical heaters. The method is used to control the resonant frequency of InAs quantum dots strongly coupled to GaAs photonic crystal resonators. This technique enables independent control of large ensembles of photonic devices located on the same chip at tuning speed as high as hundreds of kilohertz. © 2009 American Institute of Physics. [DOI: 10.1063/1.3189081]

Integrated devices composed of optical resonators and waveguides are seen as one of the most promising solutions for future optical networks for information processing.<sup>1</sup> One of the main drawbacks of using resonators is that their frequencies are highly sensitive to fabrication errors, and any fluctuations in the environment that lead to changes in the index of refraction or device geometry. The complexity of designing these systems increases even more when resonators need to be coupled to single optical emitters, as is the case for devices used in quantum information science. One possible solution is to develop system capabilities where the resonators can be controlled reversibly and on an individual basis. Some of the most scalable methods for local tuning are based on controlling the index of refraction via carrier injection<sup>2,3</sup> or by changing the temperature.<sup>4,5</sup> Other tuning techniques for photonic crystals rely on gas condensation,<sup>6,7</sup> digital etching,<sup>8</sup> or local oxidation of the photonic crystal membrane.<sup>9</sup> Generally, the local control of temperature is slower than the carrier recombination, so it is preferable to use temperature for device tuning and carrier control for other functions, such as optical switching. We have already reported a method to locally control the temperature of photonic crystal devices by heating using a laser beam.<sup>4</sup> This method allows for reliable control of individual devices located on the same chip, but for large networks of resonators it is preferable that the tuning is done electrically. In this letter we demonstrate local tuning of photonic crystal devices using micron-scale electrical heaters. Although this technique primarily targets the tuning of quantum dots (QDs) and photonic crystal cavities in optical networks for quantum information science, the method can be applied to any type of optical networks where local control of temperature is desirable for tuning purposes.<sup>10</sup>

To integrate local heaters with the QD/photonic crystal structures, we designed the device shown in Fig. 1(a). The concept of the device is similar to the one in Ref. 4, and it consists of a GaAs photonic crystal cavity next to a heating pad, both suspended via six narrow bridges to increase the thermal insulation. The device is fabricated in a 160-nm-thick GaAs membrane with a midlayer of InAs QDs, grown on top of a 1- $\mu\text{m}$ -thick AlGaAs slab that can be wet etched in hydrofluoric acid. The photonic crystal and the heating pad cover a  $11 \times 5 \mu\text{m}^2$  area. The left suspension bridges in Fig. 1(a) were 2  $\mu\text{m}$  long and 1  $\mu\text{m}$  wide, while the others

were 2  $\mu\text{m}$  long and 0.55  $\mu\text{m}$  wide. First, the photonic crystal devices were fabricated in the GaAs membrane using electron-beam lithography and dry plasma etching. Then the Ohmic heaters and the contact pads were patterned using a second lithography step followed by metal deposition and lift-off. In the last fabrication step, the AlGaAs substrate was underetched using hydrofluoric acid (6%).

The temperature control is achieved via micron-scale Ohmic heaters located on the heating pad. The heaters were first patterned by electron-beam lithography and then two metal layers (15 nm Au on top of 20 nm Cr) were deposited. A serpentine shape was chosen in order to increase the resistance of the device. Multiple devices on the same chip can be electrically connected [Figs. 1(b) and 1(c)]. The devices were connected in series in sets of eight, with four devices being

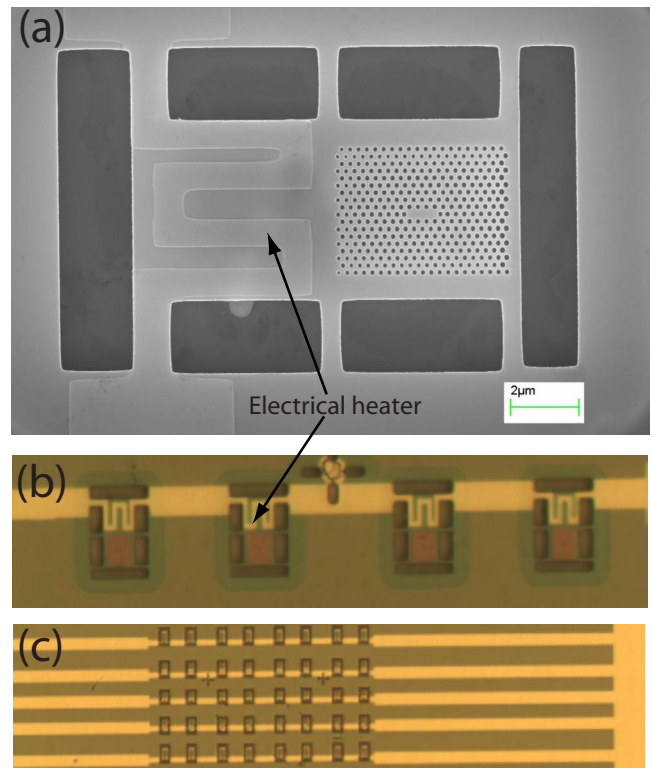


FIG. 1. (Color online) (a) Scanning electron microscope image of the suspended GaAs photonic crystal cavity and the heating pad. The serpentine pattern on the heating pad is the Ohmic heater. [(b) and (c)] Optical microscope images showing multiple devices interconnected electrically.

<sup>a)</sup>Electronic mail: faraon@stanford.edu.

shown in Fig. 1(b). Twenty sets were connected in parallel to two bonding pads, that were wired to an electrical power supply. The total resistance of the chip was  $\sim 80 \Omega$ , implying a resistance of  $\sim 200 \Omega$  for each individual heater.

The device was cooled down in a He flow cryostat and kept at a base temperature of 5 K, such that photoluminescence from single QDs could be observed. The measurements were performed using a confocal microscope setup and a laser tuned above the band gap of GaAs to excite photoluminescence.<sup>11</sup> Electrical control was achieved by connecting the entire chip to a function generator. The photoluminescence from a coupled cavity/QD system was monitored while the voltage was linearly changed from 0 to 1.2 V, as shown in Figs. 2(a)–2(d). Redshift of the QD and cavity frequency is observed while increasing the bias voltage. Both the cavity and the QD frequency shift show a quadratic dependence on the applied bias voltage. Figure 2(e) shows the linear shift in the QD with the square of the driving voltage (proportional to the dissipated power), in agreement with previous results in Ref. 4. To obtain the tuning range ( $\sim 0.8$  nm) shown in Fig. 2, corresponding to a temperature increase from 5 to  $\sim 25$  K, a thermal power of  $\sim 0.1$  mW was dissipated in the device.

Anticrossing was observed as one of the QD lines is tuned into resonance with the cavity, thus indicating strong coupling.<sup>12,4</sup> A fit to the data indicated a cavity quality factor  $Q \sim 13\,000$  and a QD/cavity coupling rate  $g/2\pi \sim 17$  GHz. For this particular cavity/QD system, a triplet of spectral lines was observed when the cavity is tuned into resonance with the QD. For most of the strongly coupled systems measured and fabricated in our laboratory under similar conditions, we did not observe this triplet of spectral lines. The side spectral lines correspond to the cavity/QD polaritons, while the middle spectral line should correspond to the cavity being populated with photons from other neighboring QDs. The coupling mechanism between the neighboring QDs and the cavity mode may be caused by spectral dephasing, as discussed in Ref. 13 where the spectrum of a single QD coupled to a cavity was investigated. QD blinking may be another reason for observing the triplet of spectral lines.

The data in Fig. 2 shows the tuning of the QD only over the spectral interval where the cavity/QD anticrossing can be observed. However, we emphasize that using this technique the temperature of the device can be increased up to the GaAs melting point. The maximum tuning range for this type of QDs is  $\sim 1.8$  nm, when the temperature is changed from  $\sim 4$  to  $\sim 50$  K.<sup>4</sup> The optical properties of the QD (especially wavelength and dephasing rate) depend on the local temperature of the device as shown in similar experiments where the temperature of the entire cryostat was controlled.<sup>14</sup> The dephasing rate of the QDs is an important factor since it limits the coherence of the system. Since this tuning technique enables temperature control over the entire relevant range for QD operation, the operating temperature can be precisely set such that the QD dephasing is within the parameters acceptable for any particular experiment or application.

For some applications, where fast fluctuations of the environment cause rapid changes in the cavity resonance, the maximum tuning speed is a relevant parameter. The maximum speed achievable with this tuning technique is limited by the thermal relaxation time of the device  $\tau$ . The thermal

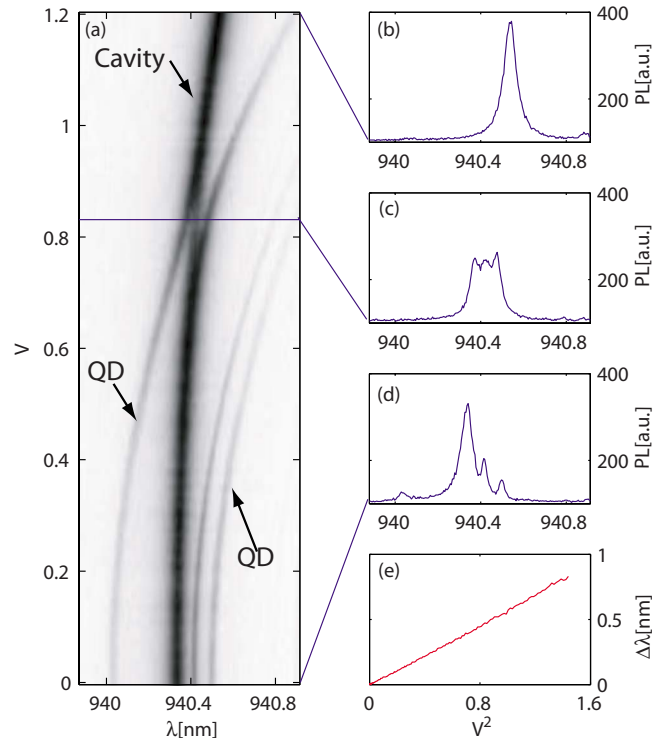


FIG. 2. (Color online) [(a)–(d)] QD and cavity tuning performed by controlling the temperature of the device using local electrical heating. Anticrossing is observed as the QD is tuned into resonance with the cavity, a signature of the strong coupling regime. (e) Linear dependence of the shift in the QD frequency with the square of the applied voltage.

relaxation time was inferred by measuring the frequency response. A device similar to the one shown in Fig. 1(a) was used for this measurement. During the experiment, the optical pump power was high enough such that the Lorentzian shape of the cavity was the dominant feature in the photoluminescence spectrum. The system was driven using a square wave (0–2 V) and the frequency was continuously swept from 10 Hz to 1 MHz. At the same time, the photoluminescence spectrum was monitored on a spectrometer at a refresh rate much slower than the modulation frequency. For modulation rates much slower than the thermal relaxation rate, the temperature of the device could follow precisely the square wave form of the driving signal, so the temperature was either  $T_0 \sim 5$  K or  $T_1 \sim 60$  K corresponding to 0 or 2 V. The spectrometer showed two resonances corresponding to the cavity frequency for the two different temperatures ( $T_0$  and  $T_1$ ). As the frequency is increased beyond the thermal relaxation rate, the temperature of the device could not follow the electrical modulation and it stabilized at the temperature corresponding to the average dissipated power. The experimental data is shown in Fig. 3 indicating that the device can be driven up to  $\sim 100$  kHz ( $\tau \sim 10$   $\mu$ s). Depending on the application, the speed of the device can be increased by using thicker suspension bridges thus increasing thermal conductivity. However, this comes at extra energy cost since more power needs to be dissipated in order to keep the device temperature at the desired level. For some applications the use of suspended structures may not be required. This could be the case for silicon on insulator devices, where the silicon oxide substrate has low thermal conductivity.

In conclusion, we show that the temperature of suspended photonic crystal devices can be controlled electri-

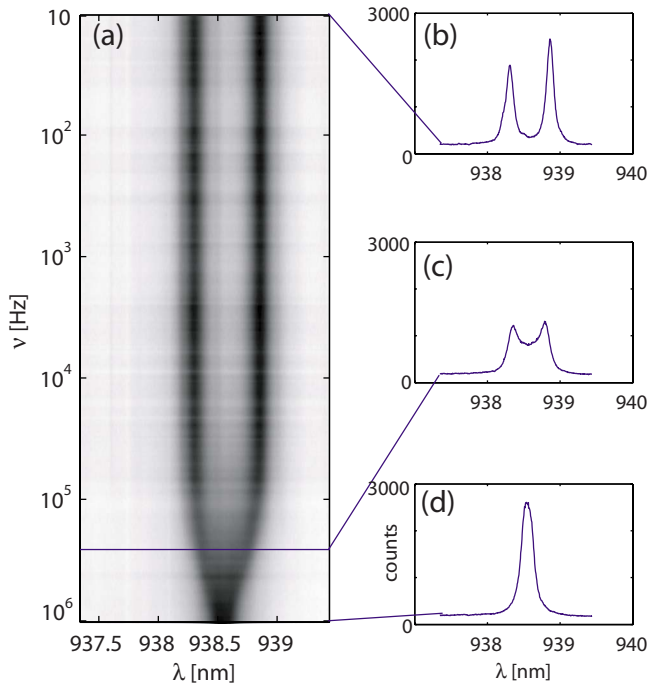


FIG. 3. (Color online) (a) Photoluminescence spectra integrated over 1 s as the temperature is tuned via a square wave signal from 10 Hz to 1 MHz. [(b)–(d)] Spectra showing three different regimes of operation. (b) Thermal relaxation rate ( $\Gamma$ ) much faster than the driving frequency ( $\omega$ ). (c)  $\Gamma \sim \omega$ . (d)  $\Gamma < \omega$ .

cally via micron-scale electrical heaters. This would enable efficient tuning of large ensembles of photonic crystal devices located on the same chip. Tuning speeds up to 100 kHz are demonstrated, limited by the thermal relaxation time of the device.

Financial support was provided by the ONR Young Investigator Award, Presidential Early Career Award, Army Research Office. Part of the work was performed at the Stanford Nanofabrication Facility of NNIN supported by the National Science Foundation, Grant No. ECS-9731293. The authors thank Professor Pierre Petroff and Dr. Nick Stoltz for providing the GaAs material.

- <sup>1</sup>S. Noda, *J. Lightwave Technol.* **24**, 4554 (2006).
- <sup>2</sup>A. Laucht, F. Hofbauer, N. Hauke, J. Angele, S. Stobbe, M. Kaniber, G. Böhm, P. Lodahl, M. C. Amann, and J. J. Finley, *New J. Phys.* **11**, 023034 (2009).
- <sup>3</sup>Q. Xu, B. Schmidt, S. Pradhan, and M. Lipson, *Nature (London)* **435**, 325 (2005).
- <sup>4</sup>A. Faraon, D. Englund, I. Fushman, N. Stoltz, P. Petroff, and J. Vučković, *Appl. Phys. Lett.* **90**, 213110 (2007).
- <sup>5</sup>M. S. Nawrocka, T. Liu, X. Wang, and R. R. Panepucci, *Appl. Phys. Lett.* **89**, 071110 (2006).
- <sup>6</sup>S. Mosor, J. Hendrickson, B. C. Richards, J. Sweet, G. Khitrova, H. M. Gibbs, T. Yoshie, A. Scherer, O. B. Shchekin, and D. G. Deppe, *Appl. Phys. Lett.* **87**, 141105 (2005).
- <sup>7</sup>S. Strauf, M. T. Rakher, I. Carmeli, K. Hennessy, C. Meier, A. Badolato, M. J. A. DeDood, P. M. Petroff, E. L. Hu, E. G. Gwinn, and D. Bouwmeester, *Appl. Phys. Lett.* **88**, 043116 (2006).
- <sup>8</sup>K. Hennessy, A. Badolato, A. Tamboli, P. M. Petroff, E. Hu, M. Atatüre, J. Dreiser, and A. Imamoglu, *Appl. Phys. Lett.* **87**, 021108 (2005).
- <sup>9</sup>K. Hennessy, C. Högerle, E. Hu, A. Badolato, and A. Imamoglu, *Appl. Phys. Lett.* **89**, 041118 (2006).
- <sup>10</sup>M. R. Wang, H.-Y. Ng, D. Li, X. Wang, J. Martinez, R. R. Panepucci, and K. Pathak, *Nanoengineering, Fabrication, Properties, Optics, and Devices IV*, Proceedings of SPIE, edited by E. A. Dobisz and L. A. Eldada (2007), Vol. 6645, p. 66450I.
- <sup>11</sup>D. Englund, A. Faraon, I. Fushman, N. Stoltz, P. Petroff, and J. Vučković, *Nature (London)* **450**, 857 (2007).
- <sup>12</sup>T. Yoshie, A. Scherer, J. Hendrickson, G. Khitrova, H. Gibbs, G. Rupper, C. Ell, O. Shchekin, and D. Deppe, *Nature (London)* **432**, 200 (2004).
- <sup>13</sup>K. Hennessy, A. Badolato, M. Winger, D. Gerace, M. Atatüre, S. Gulde, S. Falt, E. Hu, and A. Imamoglu, *Nature (London)* **445**, 896 (2007).
- <sup>14</sup>M. Bayer and A. Forchel, *Phys. Rev. B* **65**, 041308 (2002).